

## Classification of the interlayer coupling in high- $T_c$ cuprates from low-field magnetization studies

N. E. Hussey, J. R. Cooper,\* R. A. Doyle, C. T. Lin,† W. Y. Liang, and D. C. Sinclair‡  
*Interdisciplinary Research Centre in Superconductivity, University of Cambridge, Madingley Road,  
 Cambridge, CB3 0HE, United Kingdom*

G. Balakrishnan and D. McK. Paul  
*Department of Physics, University of Warwick, CV4 7AL, United Kingdom*

A. Revcolevschi  
*Laboratoire de Chimie des Solides, Université Paris Sud, 91405 Orsay Cedex, France*  
 (Received 21 August 1995)

Low-field magnetization  $M(H)$  measurements are reported for single crystals of various high- $T_c$  cuprates with different anisotropies ( $\gamma = \lambda_c / \lambda_{ab}$ , where  $\lambda_c$  and  $\lambda_{ab}$  are the  $c$ -axis and  $ab$ -plane penetration depths). For  $\text{YBa}_2\text{Cu}_3\text{O}_7$  ( $\gamma \approx 5$ ) and  $\text{La}_{1.89}\text{Sr}_{0.11}\text{CuO}_4$  ( $\gamma \approx 12$ ), qualitatively similar  $M(H)$  behavior is observed when the magnetic field is applied both perpendicular ( $H \parallel c$ ) and parallel ( $H \parallel ab$ ) to the  $\text{CuO}_2$  planes, consistent with a description of these compounds as anisotropic three-dimensional superconductors.  $\text{Tl}_2\text{Ba}_2\text{CuO}_{6+\delta}$  ( $\gamma \approx 25$ ) and  $\text{Bi}_2\text{Sr}_2\text{CaCu}_2\text{O}$  ( $\gamma \approx 250$ ), on the other hand, show significant differences in  $M(H)$  with  $H \parallel ab$  which can be attributed to the presence of Josephson screening currents across the layers. These observations imply that the nature of the interlayer coupling is determined primarily by the ratio of the out-of-plane coherence length  $\xi_c$  to the interlayer spacing  $s$ .

### I. INTRODUCTION

In high- $T_c$  cuprates, the superconducting layers are weakly coupled along the crystalline  $c$  axis leading to strong anisotropy in their physical properties. In many anisotropic layered superconductors, the phase of the superconducting order parameter is continuous across the layers and anisotropic three-dimensional (3D) Ginzburg-Landau theory is applicable. However, when the coupling is sufficiently weak, the interlayer phase difference becomes discrete and the free energy must be expressed in terms of the Lawrence-Doniach formulas for a Josephson-coupled multilayered superconductor.<sup>1</sup> There is significant evidence<sup>2</sup> that in the strongly anisotropic cuprate  $\text{Bi}_2\text{Sr}_2\text{CaCu}_2\text{O}_8$  ( $\gamma \approx 250$ ), the layers are Josephson coupled, while at the other extreme,  $\text{YBa}_2\text{Cu}_3\text{O}_7$  ( $\gamma \approx 5$ ) can be described adequately using an anisotropic 3D approach.<sup>3</sup> For intermediate anisotropies, however, the nature of the interlayer coupling has not yet been systematically studied though recent experiments have suggested that some of these compounds possess various properties attributable to intrinsic Josephson effects. For example,  $\text{Tl}_2\text{Ba}_2\text{CuO}_6$  (Ref. 4) ( $\gamma \approx 25$ ) and  $\text{Nd}_{1.85}\text{Ce}_{0.15}\text{CuO}_4$  (Ref. 5) ( $\gamma \approx 30$ ), show large discontinuities in the magnetization at fields close to  $H_{c1}$  when the field is applied parallel to the  $ab$  planes. This discontinuity is thought to arise from the destruction of Josephson screening currents between the layers by the magnetic field. In  $\text{La}_{2-x}\text{Sr}_x\text{CuO}_4$  ( $\gamma \approx 12$ ), the  $c$ -axis penetration depth  $\lambda_c$  is reported<sup>6</sup> to follow a temperature dependence similar to the Ambegaokar-Baratoff relation for Josephson junctions and a recent model<sup>7</sup> involving thermal fluctuations of the phase of Josephson junctions between the planes has been successful in modeling the  $c$ -axis resistive transition of  $\text{La}_{2-x}\text{Sr}_x\text{CuO}_4$  with  $H \parallel c$  (the quasi-force-free configuration). However, in all these intermediately an-

isotropic systems, no direct evidence has yet been reported for intrinsic Josephson coupling.

The presence of  $c$ -axis Josephson screening currents has a profound effect on the physical behavior of a layered superconductor, particularly in the mixed state, and it is therefore essential to determine the nature of the interlayer coupling for a particular cuprate system in order to understand its physical properties. Furthermore, it has been suggested recently<sup>8</sup> that only  $\lambda_c(T)$ , and not the more widely measured in-plane penetration depth  $\lambda_{ab}(T)$ , can give information regarding the orbital symmetry of the order parameter in high- $T_c$  cuprates. However, if the  $\text{CuO}_2$  layers are Josephson coupled, this should affect the temperature dependence of  $\lambda_c(T)$  in an entirely different way to nodes in the energy gap.

Low-field magnetization measurements have not been used extensively in the study of Josephson effects in high- $T_c$  single crystals, despite having various advantages over other investigative techniques. They are simple to perform and, in contrast to transport ( $I$ - $V$ ) measurements, are not prone to the problem of internal heating.<sup>9</sup> When a magnetic field is applied parallel to the superconducting layers, circulating supercurrents flow within the  $ab$  planes and also tunnel between them. If the layers are Josephson coupled, these currents will be different to ordinary London screening currents, particularly once vortices start to penetrate within the junctions. We show here that a magnetization measurement in low fields is a sensitive probe of the nature of the screening currents and the interlayer coupling in cuprate superconductors. Our procedure has been applied to a range of systems including  $\text{Bi}_2\text{Sr}_2\text{CaCu}_2\text{O}_8$ ,  $\text{Tl}_2\text{Ba}_2\text{CuO}_{6+\delta}$ ,  $\text{YBa}_2\text{Cu}_3\text{O}_7$ ,  $\text{La}_{1.89}\text{Sr}_{0.11}\text{CuO}_4$ , and the layered dichalcogenide  $\text{NbSe}_2$  ( $\gamma \approx 3$ ).

For the more anisotropic systems,  $\text{Bi}_2\text{Sr}_2\text{CaCu}_2\text{O}_8$  and  $\text{Tl}_2\text{Ba}_2\text{CuO}_{6+\delta}$ , distinct qualitative differences are ob-

TABLE I. Values of  $T_c$ ,  $\gamma$ ,  $\lambda_c(0)$ ,  $\xi_c(0)$ ,  $s$ ,  $\xi_c(0)/s$ , and  $2\xi_c(0)/(s-2.8)$  for the single crystals described in the text.  $s$  for  $\text{YBa}_2\text{Cu}_3\text{O}_7$  and  $\text{Bi}_2\text{Sr}_2\text{CaCu}_2\text{O}_8$  are taken as the larger interplanar distance.

	$T_c$ (K)	$\gamma$	$\lambda_c(0)$ ( $\mu\text{m}$ )	$\xi_c(0)$ ( $\text{\AA}$ )	$s$ ( $\text{\AA}$ )	$\xi_c/s$	$2\xi_c /$ $(s-2.8)$
$\text{Bi}_2\text{Sr}_2\text{CaCu}_2\text{O}_8$	89	>60	>15	<0.5	12.3	<0.06	<0.1
$\text{Tl}_2\text{Ba}_2\text{CuO}_6$	82	25	2	2	11.5	0.17	0.45
$\text{Tl}_2\text{Ba}_2\text{CuO}_{6+\delta}$	65	20	2	2	11.5	0.17	0.45
$\text{La}_{1.89}\text{Sr}_{0.11}\text{CuO}_4$	27	12	5	3	6.6	0.45	1.6
$\text{YBa}_2\text{Cu}_3\text{O}_7$	92	5	0.7	3.2	8.2	0.38	1.2
$\text{NbSe}_2$	7	3	1.5	30	6.0	5.0	19

served for the two orientations  $H\parallel ab$  and  $H\parallel c$ . It should be noted here that for  $H\parallel c$ , identical behavior is observed for all systems studied, showing that the differences which are found for  $H\parallel ab$  are purely a consequence of the  $c$ -axis screening currents, which we ascribe to the presence of Josephson-coupled planes in the Tl- and Bi-based compounds. On the other hand, the  $\text{YBa}_2\text{Cu}_3\text{O}_7$ ,  $\text{La}_{1.89}\text{Sr}_{0.11}\text{CuO}_4$ , and  $\text{NbSe}_2$  crystals exhibit similar magnetization behavior for both field orientations and can therefore be described as anisotropic 3D superconductors. Despite the similarity in the anisotropy of  $\text{Tl}_2\text{Ba}_2\text{CuO}_{6+\delta}$  and  $\text{La}_{1.89}\text{Sr}_{0.11}\text{CuO}_4$ , their magnetization behavior is fundamentally different. This particular observation helps clarify what parameters determine the nature of the interlayer coupling in the high- $T_c$  cuprates.

## II. EXPERIMENT

The single crystals used in this study were grown using either the floating zone method,<sup>10,11</sup> or self-flux methods.<sup>12,13</sup> All crystals were first characterized to ensure that they were fully superconducting, displaying the full screening signal with  $H\parallel ab$ , and that their transitions were sharp, with typical transition widths (10–90 %) of less than 2 K. Several crystals of each compound were investigated to check the consistency of the  $M(H)$  results (except  $\text{NbSe}_2$ ). The onset  $T_c$  for each crystal described in the text are recorded in Table I. The magnetization measurements were performed using a Cryogenic Consultants low-field SQUID susceptometer with a scan length of 5 cm. Crystals were reliably mechanically stabilized to prevent them moving in the applied field. For both field orientations, the  $M(H)$  sweeps were performed using the same procedure. Initially, each crystal was zero-field cooled ( $\leq 0.004$  G) through the transition to a set temperature to achieve an initial superconducting state with no trapped flux. The field was increased in small steps (typically  $\leq 1$  G) to beyond the field of first flux penetration and then decreased in similar sized steps to zero.<sup>14</sup> The sweep sequence was subsequently repeated, with identical or similar step sizes, but now with trapped flux, i.e., with vortices initially present within the sample. This procedure was carried out at several temperatures, though only selected field sweeps are described in the text. None of the  $M(H)$  data shown here are corrected for demagnetization factors but these are negligibly small for  $H\parallel ab$  and even for  $H\parallel c$ , they do not change any of the qualitative features that are dis-

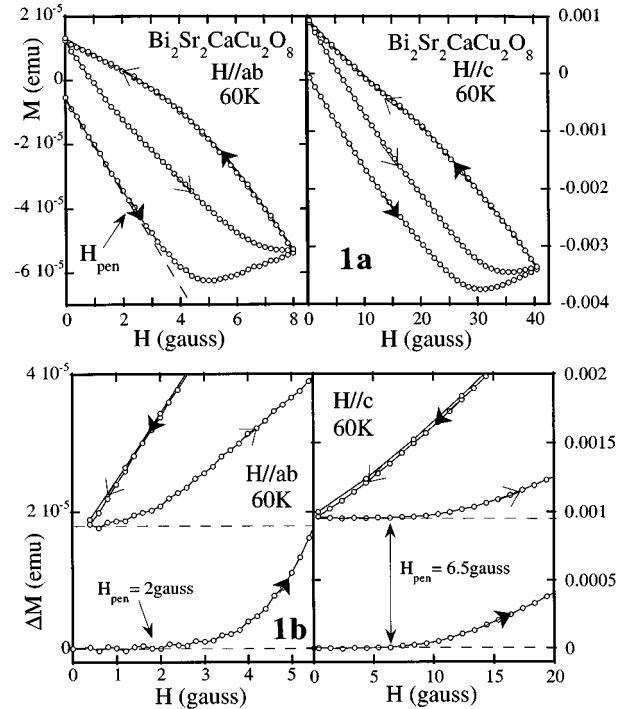


FIG. 1. (a) Consecutive  $M(H)$  curves on a  $\text{Bi}_2\text{Sr}_2\text{CaCu}_2\text{O}_8$  single crystal with  $H\parallel ab$  (left panel) and  $H\parallel c$  (right panel) at 60 K. The thick (thin) arrows indicate the direction of the first- (second-) field sweep. The dotted line represents the Meissner screening signal and  $H_{\text{pen}}$  is the field of first flux penetration. (The same convention is adopted throughout this paper.) (b) Deviation of the magnetization from the Meissner signal  $\Delta M(H) = M(H) - \chi_M H$  [where  $\chi_M$  is the slope of the linear (Meissner) region] for the magnetization curves shown in (a). For  $H\parallel ab$ ,  $\chi_M = -1.40 \times 10^{-5}$  emu/G and for  $H\parallel c$ ,  $\chi_M = -1.75 \times 10^{-4}$  emu/G.

cussed. There have been reports recently of the presence of geometrical barriers in high- $T_c$  cuprates, which can have a profound effect on the magnetization behavior with  $H\parallel c$ .<sup>17</sup> However, geometrical barriers are not thought to influence our findings, since the anomalous behavior is only found with  $H\parallel ab$  and in all crystals studied, including  $\text{NbSe}_2$ , the magnetization behavior with  $H\parallel c$  show essentially the same features.

## III. RESULTS

### A. $\text{Bi}_2\text{Sr}_2\text{CaCu}_2\text{O}_8$

Figure 1(a) shows a typical  $M(H)$  loop for  $\text{Bi}_2\text{Sr}_2\text{CaCu}_2\text{O}_8$  with  $H\parallel ab$  (left panel) and  $H\parallel c$  (right panel) at a temperature  $T=60$  K. The initial linear region on the first sweep (marked by a thick arrow) represents the Meissner signal and deviations from the dotted line correspond to flux penetration into the crystal. The field at which flux starts to penetrate is labeled  $H_{\text{pen}}$ . The peak in  $M(H)$  on the first sweep was observed at all temperatures. Moreover, there was no indication of any further increase in magnetization beyond the peak, thus confirming that the alignment parallel to the planes was good.<sup>15,16</sup> The raw  $M(H)$  data look very similar in both cases, except for the difference in scales. In order to study the field evolution of the internal flux density with field more closely, the magnetization data have been plotted

in Fig. 1(b) as  $\Delta M(H) = M(H) - \chi_M H$ , where  $\chi_M$  is the slope of the linear (Meissner) region. In these plots, an important difference is revealed in the low-field behavior of the magnetization for the two field orientations. With  $H \parallel c$ , the initial behavior of  $\Delta M(H)$  is the same for both field sweeps, i.e., no flux penetration takes place below  $H = H_{\text{pen}}$ , even though vortices are already present within the crystal at the start of the second sweep. With  $H \parallel ab$ , however, the internal flux density changes for all  $H > 0$  on the second sweep but not on the first one.

In order to understand this fundamental difference in behavior, it is important to take into account the very weak nature of the interlayer coupling in this highly anisotropic material and picture the layered structure of  $\text{Bi}_2\text{Sr}_2\text{CaCu}_2\text{O}_8$  as a stack of Josephson junctions.<sup>2</sup> It is well known that the presence of a magnetic field within a Josephson junction causes strong suppression of the Josephson currents across it because of its influence on the phase of the order parameter.<sup>18</sup> Furthermore, it has been shown theoretically<sup>19,20</sup> that when a magnetic field exceeding  $H_{c1}$  is applied parallel to the layers of a weakly Josephson-coupled layered superconductor, Josephson vortices begin to form within the layers, the surface currents are effectively suppressed and there is no further screening of the parallel component of the external field. Thus, at the start of the second sweep, with vortices still present between the  $\text{CuO}_2$  planes, no screening is possible and the magnetization changes as soon as the applied field is stepped up again. By contrast, with  $H \parallel c$ , the  $ab$ -plane supercurrents have no Josephson component and the system behaves as a conventional type-II superconductor, with surface currents coexisting alongside the vortices.<sup>21</sup> These surface currents screen further flux penetration on the second sweep until  $H_{\text{pen}}$  is reached once more.

A second fundamental difference between the two field directions is the actual field dependence of the internal flux density beyond  $H_{\text{pen}}$ . In Fig. 2,  $\Delta M$  is plotted against  $(H - H_{\text{pen}})^2$  to compare  $\Delta M(H)$  with the classical Bean critical state behavior for a constant- $J_c$  flux profile.<sup>22,23</sup> With  $H \parallel c$ ,  $\Delta M(H)$  for both the first- and second-field sweeps follows the expected  $(H - H_{\text{pen}})^2$  behavior, the rate of flux entry being lower on the second sweep due to the presence of the trapped flux. For  $H \parallel ab$ , however,  $\Delta M$  on the first sweep follows no simple field dependence just beyond  $H_{\text{pen}}$ , though it varies as  $(H - H_{\text{pen}})^2$  at higher fields [above  $(H - H_{\text{pen}})^2 \approx 10$ ]. On the second sweep,  $\Delta M \propto (H - H_{\text{pen}})^2$  for all  $H > 0$ . The unusual variation of  $\Delta M(H)$  just above  $H_{\text{pen}}$  on the first sweep can also be understood within the Josephson picture if the  $\text{CuO}_2$  planes are assumed to have a broad, continuous distribution of Josephson coupling strengths. At  $H_{\text{pen}}$ , vortices begin to penetrate only into junctions with the lowest critical currents and fields, then as the applied field is increased further, the variation of  $\Delta M(H)$  reflects the spread of critical currents (fields) of the individual junctions. Further support for such a scenario in  $\text{Bi}_2\text{Sr}_2\text{CaCu}_2\text{O}_8$  was reported recently<sup>24</sup> from  $c$ -axis current-voltage ( $I$ - $V$ ) characteristics with  $H \parallel c$  ( $H = 2$  T). In this report, sharp  $I$ - $V$  characteristics were observed over a narrow temperature range ( $14 < T < 25$  K) which was believed to represent phase locking of the individual junctions in the magnetic field. As the temperature was lowered, differences in the physical properties of the individual junctions began to

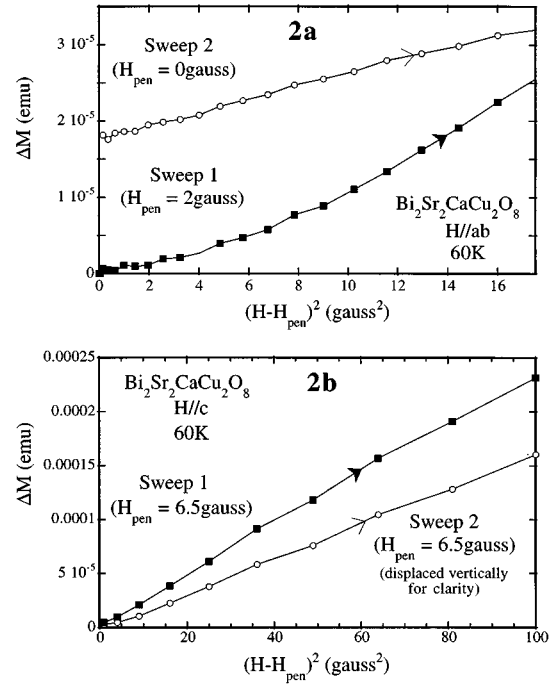


FIG. 2.  $\Delta M$  vs  $(H - H_{\text{pen}})^2$  for  $H \parallel ab$  (a) and for  $H \parallel c$  (b) for  $\text{Bi}_2\text{Sr}_2\text{CaCu}_2\text{O}_8$  at  $T = 60$  K. For  $H \parallel c$ ,  $H_{\text{pen}}$  is the same for both field sweeps and for clarity the data on the second sweep have been shifted vertically, whereas for  $H \parallel ab$ ,  $H_{\text{pen}}$  is zero on the second sweep. The values of  $H_{\text{pen}}$  used in each case are shown in the figures. For clarity, only low field data are shown.

diverge, causing the junctions to unlock. The resulting broad  $I$ - $V$  characteristic observed at lower temperatures was thus viewed as a manifestation of the continuous distribution of  $J_c$ 's along the  $c$  axis.<sup>24</sup>

Once  $H$  has exceeded the lower critical field of all the junctions,  $\Delta M(H)$  begins to follow the  $(H - H_{\text{pen}})^2$  dependence found in the other field orientation. This observation, and the quadratic behavior observed on the second sweep with  $H \parallel ab$ , suggests that the dynamics of the Josephson vortices also obey critical state behavior. This is surprising at first sight because the defect pinning mechanisms that control the dynamics of Abrikosov vortices are not expected to apply to Josephson vortices, since there are no normal cores to be pinned in the latter. However, critical state behavior of Josephson vortices was reported recently<sup>25</sup> based on magnetization measurements on  $\text{Tl}_2\text{Ba}_2\text{CuO}_{6+\delta}$  single crystals with  $H \parallel ab$ . Here it was suggested that local variations of the tunneling distance between the junctions may introduce a finite pinning of Josephson vortices moving along the  $ab$  planes. Dislocations can also act to pin Josephson vortex motion along the planes. Thus, although the inner core of Josephson and Abrikosov vortices are fundamentally different, different pinning mechanisms may give rise to similar dynamical behavior for both types of vortices in the mixed state. In addition, it was suggested in Ref. 4 that beyond  $H_{\text{pen}}$ , Josephson vortices combine to form a regular triangular lattice in a similar way to Abrikosov vortices, i.e., as elliptical current distributions with major and minor axes  $\lambda_c$  and  $\lambda_{ab}$ , respectively. Theoretical support for this picture was reported recently by Bulaevskii *et al.*<sup>26</sup> who investigated the vortex dynamics of such a multilayered system in a par-

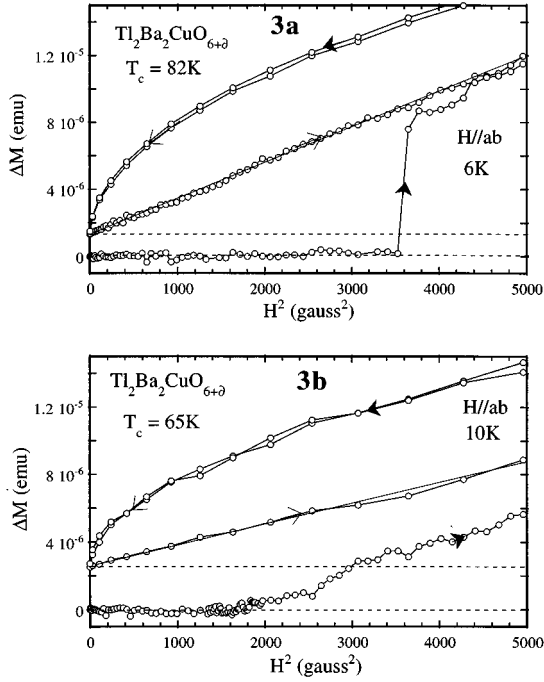


FIG. 3. (a)  $\Delta M$  vs  $H^2$  for  $\text{Tl}_2\text{Ba}_2\text{CuO}_{6+\delta}$  crystal ( $T_c = 82$  K) at  $T = 6$  K with  $H \parallel ab$  ( $\chi_M = -2.4 \times 10^{-7}$  emu/G). (b)  $\Delta M$  vs  $H^2$  for  $\text{Tl}_2\text{Ba}_2\text{CuO}_{6+\delta}$  crystal ( $T_c = 65$  K) at  $T = 10$  K with  $H \parallel ab$  ( $\chi_M = -1.8 \times 10^{-7}$  emu/G). Again, only the lowest field data are shown.

allel magnetic field. Their time-dependent phase equation for individual junctions predicts an anisotropic triangular lattice of Josephson vortices with current and field distributions almost identical to those of Abrikosov vortices.

### B. $\text{Tl}_2\text{Ba}_2\text{CuO}_{6+\delta}$

Figure 3 shows field sweeps with  $H \parallel ab$  for two  $\text{Tl}_2\text{Ba}_2\text{CuO}_{6+\delta}$  crystals with different transition temperatures plotted as deviations from the initial  $M(H)$  curves,  $\Delta M$  versus  $H^2$ . Figure 3(a) shows the data for a crystal with  $T_c = 82$  K. A large discontinuity in  $M(H)$  that was reported previously<sup>4</sup> is observed at  $H = H_{\text{pen}}$ . The discontinuity at  $H = H_{\text{pen}}$  cannot be accounted for within the Abrikosov model and has been attributed<sup>5,4,27</sup> to the magnetic decoupling of the Josephson interaction between the layers at  $H_{\text{pen}}$ .<sup>19,20</sup> On the second sweep,  $\Delta M$  varies as  $H^2$  for all finite  $H$ , and hence there is no field range in which the external field is screened once vortices are present inside the crystal, as found for  $\text{Bi}_2\text{Sr}_2\text{CaCu}_2\text{O}_8$ . Thus, apart from the discontinuous jump in  $M(H)$  in  $\text{Tl}_2\text{Ba}_2\text{CuO}_{6+\delta}$ , the magnetization behavior in  $\text{Tl}_2\text{Ba}_2\text{CuO}_{6+\delta}$  and  $\text{Bi}_2\text{Sr}_2\text{CaCu}_2\text{O}_8$  are qualitatively the same. The fact that the flux penetrates discontinuously at  $H_{\text{pen}}$  suggests that the Josephson coupling between the layers in this crystal is very well matched from layer to layer, leading to a single  $H_{c1}$  for the vast majority of junctions.  $\text{Tl}_2\text{Ba}_2\text{CuO}_{6+\delta}$  is intrinsically less disordered than  $\text{Bi}_2\text{Sr}_2\text{CaCu}_2\text{O}_8$  because of the incommensurate distortions of the BiO layers in the latter. Hence, the different

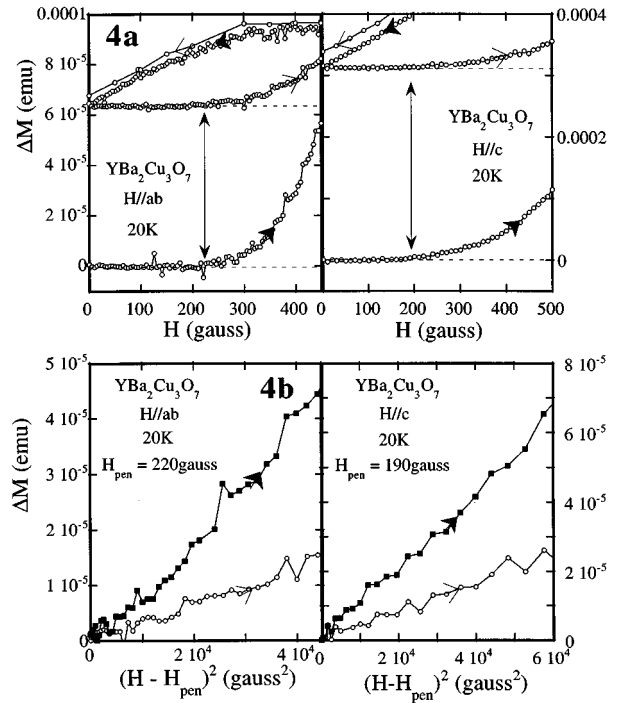


FIG. 4. (a)  $\Delta M$  vs  $H$  for  $\text{YBa}_2\text{Cu}_3\text{O}_7$  crystal at  $T = 20$  K with  $H \parallel ab$  (left panel) and  $H \parallel c$  (right panel). The double headed arrows indicate the position of  $H_{\text{pen}}$ . For  $H \parallel ab$ ,  $\chi_M = -2.40 \times 10^{-6}$  emu/G and for  $H \parallel c$ ,  $\chi_M = -1.25 \times 10^{-5}$  emu/G. (b)  $\Delta M$  vs  $(H - H_{\text{pen}})^2$  for  $H \parallel ab$  (right panel) and for  $H \parallel c$  (left panel). Only the lowest-field data are shown.

behavior of  $\Delta M(H)$  at  $H_{\text{pen}}$  can be understood and the unusual low-field magnetization behavior of both  $\text{Tl}_2\text{Ba}_2\text{CuO}_{6+\delta}$  and  $\text{Bi}_2\text{Sr}_2\text{CaCu}_2\text{O}_8$  with  $H \parallel ab$  appears to be consistent with the Josephson nature of the interlayer coupling in these two compounds.

For the lower  $T_c$  sample, shown in Fig. 3(b) ( $T_c = 65$  K), the discontinuity is absent, though all the essential features of the Josephson behavior described above are still evident. In this case,  $\Delta M(H)$  above  $H_{\text{pen}}$  shows a gradual increase with field similar to that found for  $\text{Bi}_2\text{Sr}_2\text{CaCu}_2\text{O}_8$ . To reduce  $T_c$  in  $\text{Tl}_2\text{Ba}_2\text{CuO}_{6+\delta}$ , the system must be overdoped by the addition of excess oxygen [approximately 5% per unit cell for a  $T_c$  of 65 K (Ref. 28)] which are located interstitially between the TlO layers.<sup>29</sup> This extra oxygen probably leads to greater disorder in the TlO layers and ultimately to a broader distribution of interlayer coupling strengths as in  $\text{Bi}_2\text{Sr}_2\text{CaCu}_2\text{O}_8$ . In fact, measurements on several single crystals of  $\text{Tl}_2\text{Ba}_2\text{CuO}_{6+\delta}$  with differing  $T_c$ 's reveal that, generally, the higher the  $T_c$ , the sharper the peak at  $H_{\text{pen}}$ , in agreement with this picture.

### C. $\text{YBa}_2\text{Cu}_3\text{O}_7$

Figure 4(a) shows  $\Delta M$  versus  $H$  for an optimally doped  $\text{YBa}_2\text{Cu}_3\text{O}_7$  crystal with  $H \parallel ab$  and  $H \parallel c$  at  $T = 20$  K. In contrast to the behavior found in  $\text{Tl}_2\text{Ba}_2\text{CuO}_{6+\delta}$  and  $\text{Bi}_2\text{Sr}_2\text{CaCu}_2\text{O}_8$ , the essential features of the first- and second-field sweeps are very similar for both orientations.

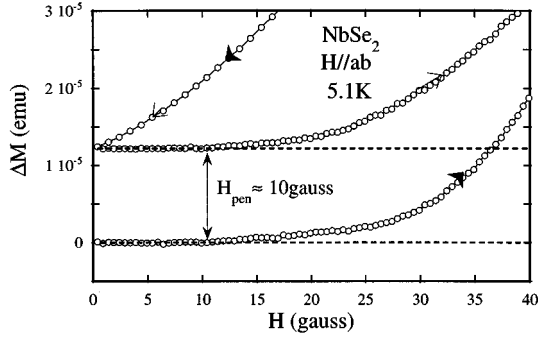


FIG. 5.  $\Delta M(H)$  curves for  $\text{NbSe}_2$  at  $T=5.1$  K with  $H\parallel ab$ . ( $\chi_M = -1.80 \times 10^{-6}$  emu/G.)

First,  $\Delta M(H)$  remains unchanged at low fields up to the same  $H_{\text{pen}}$  on both sweeps. Second, as shown in Fig. 4(b),  $\Delta M$  varies quadratically with field above  $H_{\text{pen}}$  in all cases. Thus, the screening currents flowing across the layers appear to behave in an identical fashion to those flowing within the planes and there are no signatures of Josephson coupling with  $H\parallel ab$ .  $\text{YBa}_2\text{Cu}_3\text{O}_7$  therefore seems to behave as an anisotropic three-dimensional superconductor with no Josephson interaction along the  $c$  axis. The flux lattice is presumably composed of Abrikosov vortices in both field orientations.

These results reveal how low-field magnetization measurements can be used to determine the nature of the inter-layer coupling in layered superconductors. The different behavior observed in the two field orientations for  $\text{Tl}_2\text{Ba}_2\text{CuO}_{6+\delta}$  and  $\text{Bi}_2\text{Sr}_2\text{CaCu}_2\text{O}_8$  arises from the different nature of the screening currents within the  $\text{CuO}_2$  planes and across the layers. In less anisotropic  $\text{YBa}_2\text{Cu}_3\text{O}_7$ , similar behavior is observed for both field orientations, implying that only standard (non-Josephson) screening currents, with anisotropic penetration depths, exist in this compound.

#### D. $\text{NbSe}_2$

For comparison with the cuprate superconductors, we performed identical  $M(H)$  measurements on a single crystal of the layered dichalcogenide  $\text{NbSe}_2$  [ $T_c=7$  K,  $\gamma=3$  (Ref. 30)]. Figure 5 shows the  $\Delta M(H)$  data with  $H\parallel ab$  at  $T=5.1$  K. This figure shows clearly that the behavior at low fields for both field sweeps is in fact similar to that found for  $\text{YBa}_2\text{Cu}_3\text{O}_7$ . (Identical behavior was also observed for  $H\parallel c$ , but is not shown here.) This observation, for a less anisotropic noncuprate compound, further supports the anisotropic 3D picture presented above for  $\text{YBa}_2\text{Cu}_3\text{O}_7$ .

#### E. $\text{La}_{1.89}\text{Sr}_{0.11}\text{CuO}_4$

The  $\text{La}_{1.89}\text{Sr}_{0.11}\text{CuO}_4$  crystal reported in this study has an anisotropy  $\gamma \approx 12$  determined both from the magnetization (i.e.,  $H_{c1}$  measurements and the resistivity anisotropy of a second piece of the same crystal) which is intermediate between the anisotropy of  $\text{YBa}_2\text{Cu}_3\text{O}_7$  and  $\text{Tl}_2\text{Ba}_2\text{CuO}_{6+\delta}$ . The  $\Delta M(H)$  data for  $H\parallel ab$  at  $T=18$  K are shown in Fig. 6(a). As found for  $\text{YBa}_2\text{Cu}_3\text{O}_7$  and  $\text{NbSe}_2$ ,  $\Delta M(H)$  on the second sweep is parallel with that of the first until  $H_{\text{pen}}$  and is again found to vary quadratically with  $(H-H_{\text{pen}})$  in both

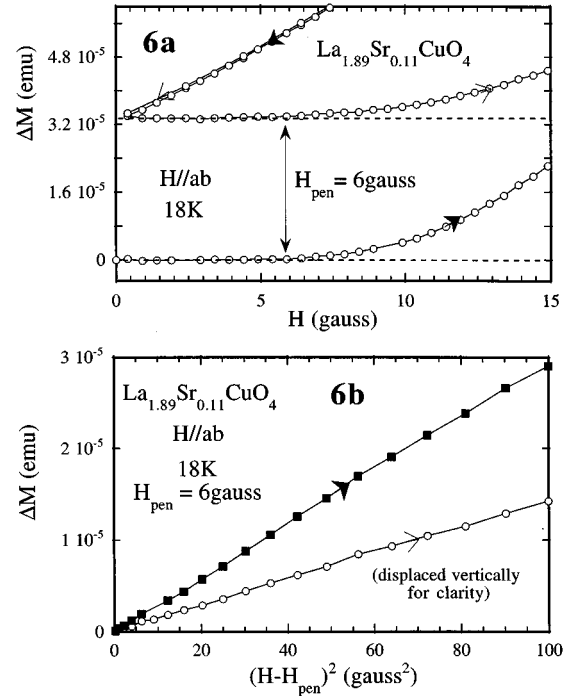


FIG. 6. (a)  $\Delta M(H)$  curves for  $\text{La}_{1.89}\text{Sr}_{0.11}\text{CuO}_4$  at  $T=18$  K with  $H\parallel ab$  (low-field data only) ( $\chi_M = -4.80 \times 10^{-6}$  emu/G). (b)  $\Delta M$  vs  $(H-H_{\text{pen}})^2$  for the same curves, the data for the second sweep have been shifted vertically.

field sweeps [see Fig. 6(b)]. Thus, it appears that  $\text{La}_{1.89}\text{Sr}_{0.11}\text{CuO}_4$  should also be considered as an anisotropic 3D superconductor.

## IV. DISCUSSION

Table I summarizes the results for all single crystals discussed in the previous section. The values of the anisotropy parameter  $\gamma$  were obtained directly from our own magnetization measurements (except  $\text{NbSe}_2$  for which  $\gamma$  was taken from the literature<sup>30</sup>). To estimate  $\gamma$ , we assume that  $H_{\text{pen}}$  (from the first field sweep) corresponds to the lower critical field,  $H_{c1}$  in each field orientation. The ratio of the penetration fields for  $H\parallel ab$  and  $H\parallel c$  must then be scaled by the demagnetization factor  $1/(1-N_c)$ , determined experimentally from the ratios of the initial linear (Meissner) regions of the  $M(H)$  data at the lowest temperature measured.<sup>15</sup> For the thin platelet samples used in this study, the demagnetization factor  $1/(1-N_c) \approx 1$  for  $H\parallel ab$ . Therefore,  $\gamma \approx (H_{\text{pen},c}/H_{\text{pen},ab})/(1-N_c)$  where  $H_{\text{pen},c}$  ( $H_{\text{pen},ab}$ ) is the penetration field measured at the lowest temperature with  $H\parallel c$  ( $H\parallel ab$ ) and  $1/(1-N_c)$  is the demagnetization factor for  $H\parallel c$ . Inspection of Table I leads us to conclude that there is some correlation between the level of anisotropy and the appearance of Josephson coupling and that the critical regime for the crossover from 3D to quasi-2D occurs in the range  $12 \leq \gamma \leq 20$ . The assumption that  $H_{c1} \approx H_{\text{pen}}$  is justified in that values for  $H_{\text{pen}}$  agree well with other experimental values of  $H_{c1}$  in the literature and with those obtained from appropriate formulas for  $H_{c1}$  (Refs. 18 and 31) using typical values of  $\lambda_{ab}$  and  $\gamma$  from the literature. This implies that for the crystals studied here, surface barriers have little or no

effect on their  $M(H)$ . The only possible exception is the  $\text{YBa}_2\text{Cu}_3\text{O}_7$  crystal where  $H_{\text{pen},ab}$  ( $= 220$  G) is a factor of 2 higher than expected for typical values of  $\gamma$  ( $= 5$ ) and  $\lambda_{ab}$  ( $= 1400$  Å). However, for two other  $\text{YBa}_2\text{Cu}_3\text{O}_7$  crystals also measured in this study (not discussed here),  $H_{\text{pen},ab}$  was found to be 110 G. All the essential features of the  $M(H)$  data described in the previous section for  $\text{YBa}_2\text{Cu}_3\text{O}_7$  were also observed for these two samples.

The  $c$ -axis penetration depth  $\lambda_c(0)$  gives an indication of the strength of the screening currents flowing across the  $\text{CuO}_2$  planes; the larger  $\lambda_c(0)$ , the smaller the  $c$ -axis  $J_c$ . It has been argued recently<sup>32</sup> that  $\lambda_c(0)$  is an important parameter in determining whether or not Josephson effects are to be found in the superconducting state and a large  $\lambda_c(0)$  is correlated with the nonmetallic behavior of the  $c$ -axis resistivity in the normal state. In Table I we have listed estimates of  $\lambda_c(0)$  derived from the values of  $H_{c1}$  and  $\gamma$  obtained from our magnetization data for each crystal (the value for  $\text{YBa}_2\text{Cu}_3\text{O}_7$  is derived assuming  $\gamma=5$  and  $\lambda_{ab}=1400$  Å). As one can see,  $\lambda_c(0)$  for  $\text{La}_{1.89}\text{Sr}_{0.11}\text{CuO}_4$  is more than twice that for both  $\text{Tl}_2\text{Ba}_2\text{CuO}_{6+\delta}$  crystals, implying that the  $c$ -axis screening currents in  $\text{La}_{1.89}\text{Sr}_{0.11}\text{CuO}_4$  are weaker than in  $\text{Tl}_2\text{Ba}_2\text{CuO}_{6+\delta}$ . However, the  $M(H)$  behavior of the former is consistent with  $\text{La}_{1.89}\text{Sr}_{0.11}\text{CuO}_4$  being an anisotropic 3D superconductor while  $\text{Tl}_2\text{Ba}_2\text{CuO}_{6+\delta}$  is Josephson coupled. Thus, it appears that the magnitude of  $\lambda_c(0)$  is not the dominant factor determining the nature of the coupling between the planes.

The next column in Table I lists the values of the zero-temperature  $c$ -axis coherence length  $\xi_c(0)$  for each system. For  $\text{Bi}_2\text{Sr}_2\text{CaCu}_2\text{O}_8$  and  $\text{NbSe}_2$ ,  $\xi_c(0)$  is derived from the expression  $\xi_c(0) = \gamma \xi_{ab}(0)$  where  $\xi_{ab}(0)$  is taken from typical values reported in the literature.<sup>33</sup> For  $\text{YBa}_2\text{Cu}_3\text{O}_7$ ,  $\text{La}_{1.89}\text{Sr}_{0.11}\text{CuO}_4$ , and  $\text{Tl}_2\text{Ba}_2\text{CuO}_{6+\delta}$ ,  $\xi_c(0)$  is estimated from the thermodynamic critical field  $H_c$  derived from specific heat measurements<sup>34</sup> and the relation  $\kappa_{ab} = 2\sqrt{2}\pi H_c \lambda_{ab}(0) \lambda_c(0) / \phi_0 = \lambda_{ab}(0) / \xi_c(0)$ . In the table, one sees that for the two single layer compounds,  $\text{La}_{1.89}\text{Sr}_{0.11}\text{CuO}_4$  and  $\text{Tl}_2\text{Ba}_2\text{CuO}_{6+\delta}$ ,  $\xi_c(0)$  values are quite similar. However, the distance  $s$  between successive  $\text{CuO}_2$  planes in  $\text{Tl}_2\text{Ba}_2\text{CuO}_{6+\delta}$  is almost twice that in  $\text{La}_{1.89}\text{Sr}_{0.11}\text{CuO}_4$ . (The values of  $s$  for each crystal structure are also listed in Table I.) Thus the ratio  $\xi_c(0)/s$ , which is essentially an indication of the dimensionality of the superconducting state at  $T=0$ , does show a correlation with the onset of Josephson coupling. The critical value falls in the range  $0.17 \leq \xi_c(0)/s \leq 0.38$ . This result is significant since it suggests that even though  $\xi_c(0)$  can be less than half the interplanar distance, the system can still be considered to be three dimensional with a continuous phase change of the order parameter across the layers. Lawrence and Doniach<sup>1</sup> state that the effective mass model breaks down when  $\xi_c \leq s$ , because in this case, most of the vortex core lies between the layers in a region of low electron density. Allowing for the fact that the  $\text{CuO}_2$  layers are approximately 2.8 Å wide (i.e., twice the van der Waals radius for oxygen), the width of the low-electron density regions between the  $\text{CuO}_2$  planes is  $s - 2.8$  Å. If the order parameter decays along the  $c$  axis within this region over a distance  $\xi_c$  from both sides, one could naively expect the variation of the or-

der parameter between the layers to change from continuous to discrete whenever  $2\xi_c \leq s - 2.8$  Å. The data summarized in the last column of Table I are consistent with this remark.<sup>35</sup>

Finally, it should be recalled that  $\xi_c$  is strongly temperature dependent. Thus, for  $\text{Tl}_2\text{Ba}_2\text{CuO}_{6+\delta}$  and  $\text{Bi}_2\text{Sr}_2\text{CaCu}_2\text{O}_8$ , there will be a temperature below  $T_c$  at which point the above inequality is no longer satisfied and the behavior should revert to that of the anisotropic 3D superconductors. In  $\text{Bi}_2\text{Sr}_2\text{CaCu}_2\text{O}_8$ , this will be very close to  $T_c$  and therefore very difficult to observe. However, for  $\text{Tl}_2\text{Ba}_2\text{CuO}_{6+\delta}$ , the inequality should be violated at much lower temperatures. Though not displayed here, it was shown in Ref. 4 that for a  $\text{Tl}_2\text{Ba}_2\text{CuO}_{6+\delta}$  sample with  $T_c = 82$  K, the signatures of Josephson coupling disappeared above 45 K. This was attributed to thermal fluctuations reducing the Josephson coupling, but the present results imply that it may also be connected with the crossover in magnetization behavior at  $2\xi_c \approx s - 2.8$  Å.

In conclusion, we have found a simple technique, using successive low-field magnetization curves, to investigate the nature of the interlayer coupling in several high- $T_c$  cuprate single crystals. Systems of low anisotropy ( $\text{YBa}_2\text{Cu}_2\text{O}_7$  and  $\text{La}_{1.89}\text{Sr}_{0.11}\text{CuO}_4$ ) show essentially the same  $M(H)$  behavior on successive cycles both for  $H\parallel ab$  and  $H\parallel c$ , implying that the screening currents flowing in and out of plane are similar in nature, albeit with anisotropic effective masses. In the more anisotropic  $\text{Tl}_2\text{Ba}_2\text{CuO}_{6+\delta}$  and  $\text{Bi}_2\text{Sr}_2\text{CaCu}_2\text{O}_8$ , however, significantly different behavior is observed with  $H\parallel ab$ , which, we believe, can only result from the different properties of the screening currents that flow across the layers, in particular, the stronger effects of trapped flux on Josephson currents. Rather surprisingly, on subsequent field sweeps, various features of the (Josephson) vortex lattice in the parallel field orientation, namely its structure and dynamics, seem to show similarities with that observed for Abrikosov vortices.

By studying systems of different anisotropy, we have been able to determine an experimental criterion defining the crossover from anisotropic 3D to quasi-2D behavior in the cuprates. Further systematic studies are envisaged to investigate the sharpness of this crossover in various compounds. Finally, it should be noted that any other layered type-II superconductor could also be investigated using the same procedure. By making successive (zero-field-cooled) field sweeps with the field applied both parallel and perpendicular to the superconducting planes, one should be able to determine whether the material is Josephson coupled or three dimensional. Such knowledge would be extremely useful for understanding its behavior in subsequent experiments.

#### ACKNOWLEDGMENTS

We wish to acknowledge helpful and stimulating discussions with Dr. J. D. Johnson and Dr. V. N. Zavaritsky and thank Dr. A. P. Mackenzie and Dr. Y. Yagil for assistance in this collaborative work. In addition, we are very grateful to Dr. D. Pilgram of Twickenham Scientific Instruments and P. D. Hunneyball for invaluable technical assistance and D. M. Astill for EPMA analysis of the  $\text{La}_{1.89}\text{Sr}_{0.11}\text{CuO}_4$  crystal. This work was supported by EPSRC.

- \*On leave from The Institute of Physics of the University of Zagreb, Croatia.
- <sup>†</sup>Present address: Max Planck Institut, Heissenbergstrasse D-1, 70569 Stuttgart, Germany.
- <sup>‡</sup>Present address: Department of Solid State Chemistry, University of Aberdeen, Aberdeen, AB9 2UE, U.K.
- <sup>1</sup>W. E. Lawrence and S. Doniach, in *Proceedings of the Twelfth International Conference on Low Temperature Physics*, edited by E. Kanda (Academic Press of Japan, Kyoto, 1971), p. 361.
- <sup>2</sup>R. Kleiner and P. Müller, Phys. Rev. B **49**, 1327 (1994).
- <sup>3</sup>P. Pugnât, G. Fillion, H. Noel, M. Ingold, and B. Barbara, Europhys. Lett. **29**, 425 (1995).
- <sup>4</sup>N. E. Hussey, A. Carrington, J. R. Cooper, and D. C. Sinclair, Phys. Rev. B **50**, 13 073 (1994).
- <sup>5</sup>F. Zuo, S. Khizroev, Xiuguang Jiang, J. L. Peng, and R. L. Greene, Phys. Rev. Lett. **72**, 1746 (1994).
- <sup>6</sup>T. Shibauchi, H. Kitano, K. Uchinokura, A. Maeda, T. Kimura, and K. Kishio, Phys. Rev. Lett. **72**, 2263 (1994).
- <sup>7</sup>K. Kadowaki, S. L. Yuan, K. Kishio, T. Kimura, and K. Kitazawa, Phys. Rev. B **50**, 7230 (1994). See also D. H. Kim, K. E. Gray, R. T. Kampwirth, J. C. Smith, D. S. Richeson, T. J. Marks, J. H. Kang, J. Talvacchio, and M. Eddy, Physica C **177**, 431 (1991).
- <sup>8</sup>R. A. Klemm and S. H. Liu, Phys. Rev. Lett. **74**, 2343 (1995).
- <sup>9</sup>R. A. Doyle *et al.* (unpublished).
- <sup>10</sup>G. Balakrishnan, D. McK. Paul, M. R. Lees, and A. T. Boothroyd, Physica C **206**, 148 (1993).
- <sup>11</sup>A. Revcolevschi and G. Dhalenne, Adv. Mater. **5**, 657 (1993).
- <sup>12</sup>R. S. Liu, S. D. Hughes, R. J. Angel, T. P. Hackwell, A. P. Mackenzie, and P. P. Edwards, Physica C **198**, 203 (1992).
- <sup>13</sup>C. T. Lin, W. Zhou, W. Y. Liang, E. Schonherr, and H. Bender, Physica C **195**, 291 (1992).
- <sup>14</sup>On connecting the magnet current leads, a current leakage from the magnet power supply meant that the lowest field attainable during a field sweep was 0.4 G not zero. However, we believe this does not affect any of the features discussed in the paper.
- <sup>15</sup>N. Nakamura, G. D. Gu, and N. Koshizuka, Phys. Rev. Lett. **71**, 915 (1993).
- <sup>16</sup>V. N. Zavaritsky and N. V. Zavaritsky, Physica C **185-189**, 1869 (1991).
- <sup>17</sup>E. Zeldov, A. I. Larkin, V. B. Geshkenbein, M. Konczkowski, D. Majer, B. Khaykovich, V. M. Vinokur, and H. Shtrikman, Phys. Rev. Lett. **73**, 1428 (1994).
- <sup>18</sup>See, for example, M. Tinkham, *Introduction to Superconductivity* (McGraw-Hill, New York, 1980).
- <sup>19</sup>P. Kes, J. Aarts, V. M. Vinokur, and C. J. van der Beek, Phys. Rev. Lett. **64**, 1063 (1990).
- <sup>20</sup>S. Theodorakis, Phys. Rev. B **42**, 10 172 (1990).
- <sup>21</sup>A similar distinction between Josephson junctions and conventional type-II superconductors has been postulated theoretically by D. -X. Chen and A. Hernando, Phys. Rev. B **49**, 465 (1994).
- <sup>22</sup>C. P. Bean, Rev. Mod. Phys. **36**, 31 (1964).
- <sup>23</sup>V. V. Moshchalkov, J. Y. Henry, C. Marin, J. Rossat-Mignod, and J. F. Jacquot, Physica C **175**, 407 (1991).
- <sup>24</sup>R. A. Doyle, J. D. Johnson, N. E. Hussey, A. M. Campbell, G. Balakrishnan, D. McK. Paul, and L. F. Cohen, Phys. Rev. B **51**, 9368 (1995).
- <sup>25</sup>F. Zuo, S. Khizroev, V. N. Kopylov, and N. N. Kolesnikov, Physica C **243**, 117 (1995).
- <sup>26</sup>L. N. Bulaevskii, M. Zamora, D. Baeriswyl, H. Beck, and J. R. Clem, Phys. Rev. B **50**, 12 831 (1994).
- <sup>27</sup>F. Zuo, S. Khizroev, Xiuguang Jiang, J. L. Peng, and R. L. Green, Phys. Rev. Lett. **73**, 3328 (1994).
- <sup>28</sup>Y. Shimakawa, Physica C **204**, 247 (1993).
- <sup>29</sup>Y. Shimakawa, Y. Kubo, T. Manako, H. Igarashi, F. Izumi, and H. Asano, Phys. Rev. B **42**, 10 165 (1990).
- <sup>30</sup>V. G. Kogan and J. R. Clem, in *Concise Encyclopedia of Magnetic and Superconducting Materials*, edited by J. E. Evetts (Pergamon Press, New York, 1992), p. 43.
- <sup>31</sup>J. R. Clem, M. W. Coffey, and Z. Hao, Phys. Rev. B **44**, 2732 (1991).
- <sup>32</sup>K. Tamasaku and S. Uchida, Physica C **235-240**, 1321 (1994).
- <sup>33</sup>For  $\xi_{ab}(0)$  of  $\text{Bi}_2\text{Sr}_2\text{CaCu}_2\text{O}_8$ , see T. T. M. Palstra, B. Batlogg, L. F. Schneemeyer, R. B. van Dover, and J. V. Waszczak, Phys. Rev. B **38**, 5120 (1988). For  $\xi_{ab}(0)$  of  $\text{NbSe}_2$ , see M. Ikebe, N. Kobayashi, K. Katagiri, and Y. Muto, Physica B **105**, 435 (1980).
- <sup>34</sup>J. W. Loram and J. M. Wade (private communication).
- <sup>35</sup>When  $\xi_c$  becomes very short, the material should no longer be considered as an anisotropic homogeneous superconductor but as a stack of superconducting layers separated by nonsuperconducting regions. Even in the latter case, however,  $\xi_c$  still represents the spatial extent of the superconducting coherence volume along the  $c$  axis.